
Online Biped Walking Pattern Generation with Contact Consistency

Hou'Yongkang*, Jian Wang*, Jianwen Wang* and Hongxu Ma*

* College of Mechatronic Engineering and Automation, National University of Defense Technology

Article Info

Article history:

Received Apr 24, 2014

Revised Oct 20, 2014

Accepted Nov 16, 2014

Keyword:

Gait pattern generation

Contact consistency

Biped robot

Point foot

Orbit energy

Task space controller

ABSTRACT

In this paper, a novel online biped walking gait pattern generating method with contact consistency is proposed. Generally, it's desirable that there is no foot-ground slipping during biped walking. By treating the hip of the biped robot as a linear inverted pendulum (LIP), a foot placement controller that takes the contact consistency into account is proposed to tracking the desired orbit energy. By selecting the hip's horizontal locomotion as the parameter, the trajectories in task space for walking are planned. A task space controller without calculating the inversion of inertial matrix is presented. Simulation experiments are implemented on a virtual 5-link point foot biped robot. The results show the effectiveness of the walking pattern generating method which can realize a stable periodic gait cycle without slipping and falling even suffering a sudden disturbance.

Copyright © 2017 Institute of Advanced Engineering and Science.

All rights reserved.

Corresponding Author:

Wenqi Hou

College of Mechatronic Engineering and Automation,

National University of Defense Technology

Deya Road 109#, Changsha, China.

Email: houwnq@126.com

1. INTRODUCTION

Biped robots have aroused much attention over the past decades. But up to now, a biped walking robot that performs as well as human has not yet been made. To some extent, it indicates that the fundamental principles of biped walking are still not fully understood[1]. Generally, in order to focus on the dynamical characters of biped walking, it is assumed that the legs are terminated in points and no actuation is considered at the stance foot [2-4]. As a result, the Zero-Moment Point(ZMP) criterion can't be used in the synthesis of walking pattern[5]. Additionally, slipping between the stance foot and ground is not expected, which means that the contact consistency should be preserved. The coupling between the actuated torques and the contact forces made the control problem a great challenge for researchers.

Different approaches are proposed in literatures to handle biped walking control. By assuming the foot-ground impact is rigid and no slipping or rebounds occurs during walking, J.W. Grizzle and E.R. Westervelt et al. proved the existence and stability of periodic orbit for biped walking on a five-link, planar prototype RABBIT[6, 7]. Sentis et al. proposed an extension of operational space controllers for floating-based robots, by projecting the operational tasks into the constraint null space, the violations between different tasks are avoided[8]. However, this approach requires the inversion of the system inertia matrix in the controller, which makes it sensitive to modeling and parameter estimation errors[9]. Based on the orthogonal decomposition of the constraint Jacobian, Michael Mistry et al. proposed an inverse dynamics algorithm for legged robots, which expresses the inverse dynamics controller independently of contact forces and only requires the kinematic terms[10]. Recently, Salman Faraji et al. used such an approach to control a planar monopod hopper in rough terrain[11].

Ludovic Righetti et al. demonstrated that the approaches of Sentis et al. and Michael Mistry et al. are equivalent in essence[12], since they (including J.W. Grizzle and E.R. Westervelt et al.) are all based on the assumption that the contact constraints, by definition, are able to apply necessary forces to maintain their consistency. However, the constraints may not hold under certain situations especially for the robot with point foot. By adding additional torques to control the contact forces, Jaeheung Park and Oussams Kahtib proposed a contact consistent control framework for humanoid robots[14]. But this approach also needs to calculate the inversion of the system inertia matrix.

In order to generate walking gait that can preserve the contact consistency, by utilizing the Linear Inverted Pendulum Model(LIPM)[15], a novel online walking gait pattern generating method is proposed in this paper, and the complete control architecture is shown in Fig.1.

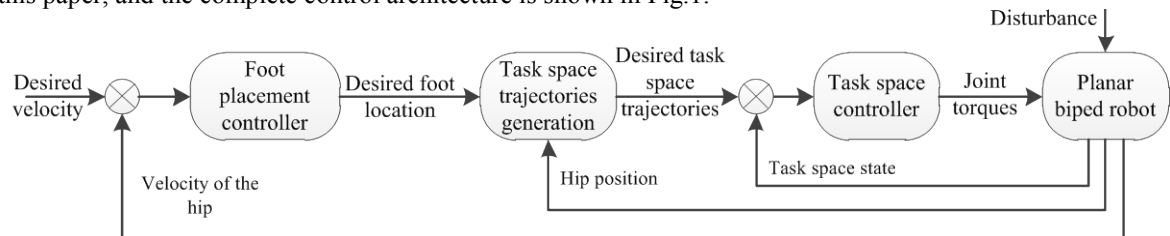


Figure 1. Block diagram for the walking control

In section 2, the relationship between the orbit energy and the foot location is discussed by analyzing the dynamics of a 2D-LIPM. With accounting for the restriction of the contact forces, a foot placement controller is proposed to track the desired orbit energy. In section 3, we discuss the generation of the desired trajectories in task space for biped walking by selecting the hip's horizontal locomotion as the parameter. In section 4, a task space controller without calculating the inversion of inertial matrix is presented. In section 5, we test the online walking pattern generating method and the task space controller on a virtual biped robot. Section 6 concludes the paper and provides the directions for future work.

2. FOOT PLACEMENT CONTROLLER WITH CONTACT CONSISTENCY

A planar 5-link point foot biped robot, as shown in Fig.2.(a), comprises two symmetric legs and a torso. From the viewpoint of natural human walking, it is desirable that the torso is always upright with minimum hip's vertical oscillation during walking. That is similar to a 2D-LIPM, which is described by Kajita et al.[15-17]. A 2D-LIPM comprises a point mass and a telescoping massless leg with a point foot, which is in contact with the flat ground, as shown in Fig.2.(c). In this paper we model the motion of the biped robot's hip as a 2D-LIPM.

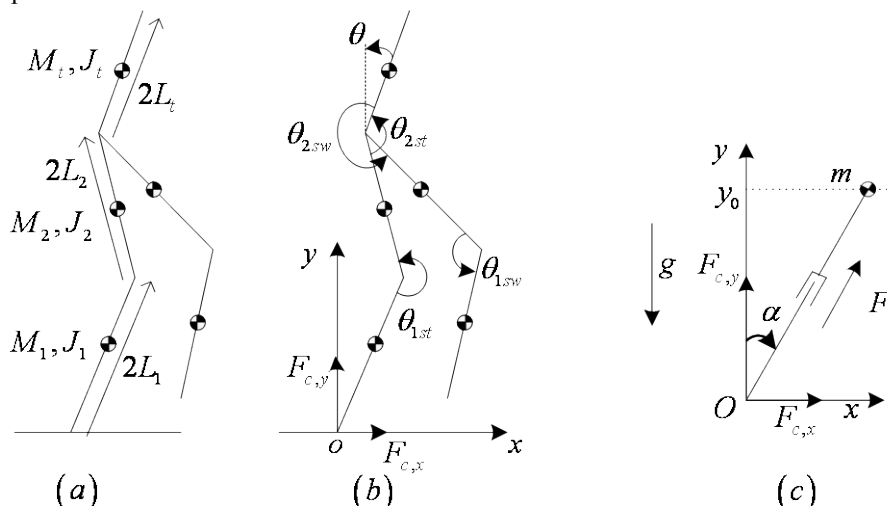


Figure 2. A planar 5-link biped robot with one foot standing on the ground: (a) physical parameters of the robot; (b) generalized coordinates; (c) a 2D-LIPM approximates the motion of the biped robot's hip. The LIPM comprised a point mass with mass m and a massless telescoping leg with point foot. The point mass is kept at constant height y_0 by an actuator that exerts a force F on it. $F_{c,x}$ and $F_{c,y}$ are the tangential and normal component of the contact force between the point foot and the ground, respectively.

2.1 2D Liner Inverted Pendulum

The equations of motion for the 2D-LIPM are[16, 17] :

$$\dot{y} = \ddot{y} = 0, y = y_0 = \text{constant} \quad (1)$$

$$\ddot{x} = g \tan \alpha = g \frac{x}{y_0} \quad (2)$$

where g is the gravitational acceleration constant, x and y are the position of the point mass, expressed in a local frame which is located at the point foot, y_0 is a constant. The orbit energy of the point mass is conserved during each stance phase, and it is defined as[15-17]:

$$E = \frac{1}{2} \dot{x}^2 - \frac{g}{2y_0} x^2 \quad (3)$$

The orbit energy determines the behavior of the LIP when the point mass is moving toward the foot. There are three cases[1]:

- $E < 0$. The point mass will stop and reverse direction before getting over the foot.
- $E = 0$. The point mass will come to a rest exactly on the foot.
- $E > 0$. The point mass will go over the foot and continue on its way.

Equation (3) indicates that the orbit energy is equivalent to the velocity when the point mass passes through the stance point. It means that with more orbit energy the point mass will move faster. So the biped walking control is an orbit energy tracking problem in essence. Additionally, Equation(3) shows that the orbit energy fully depends on the location of the foot relative to the point mass given a certain initial velocity. So the only way to change the point mass's orbit energy is changing the foot location by taking a step. To clarify the analysis better, we assume each step is taken instantaneously and the velocity of the point mass will not be affected as shown in Fig.3.

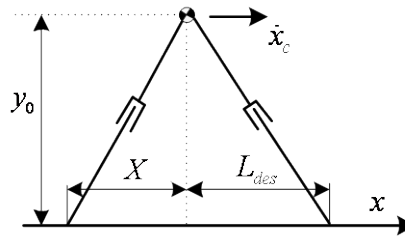


Figure 3. The moment when the 2D-LIPM is taking a step. X is the permitted maximum horizontal distance between the point mass and the foot in each stance phase, which means once the point mass arrives at $x = X$ a step must be taken. L_{des} is the horizontal distance between the desired foot location and the point mass when a step is being taken. \dot{x}_c is the velocity of the point mass at that moment.

Let E^- and E^+ be the orbit energy of the point mass before and after the 2D-LIPM takes a step, respectively, i.e.

$$E^- = \frac{1}{2} \dot{x}_c^2 - \frac{g}{2y_0} X^2 \quad (4)$$

$$E^+ = \frac{1}{2} \dot{x}_c^2 - \frac{g}{2y_0} L_{des}^2 \quad (5)$$

Equation (5) minus (4) is

$$\Delta E = E^+ - E^- = \frac{g}{2y_0} (X^2 - L_{des}^2) \quad (6)$$

Equation(6) clearly indicates that, L_{des} can change the orbit energy of the point mass for a given X , and three typical cases are included:

- $L_{des} < X$. The orbit energy will increase.
- $L_{des} = X$. The orbit energy will not change, and the point mass will move exactly as in the previous stance phase.
- $L_{des} > X$. The orbit energy will decrease.

So, in order to realize the motion of the point mass with desired orbit energy, the foot location should be properly controlled for every step.

2.2 Foot Placement Controller

For biped walking control, there are two questions to be answered: when a step should be taken? Where the foot should be placed? Here we will answer these questions by taking two practical restrictions account.

First, in order to maintain the foot-ground contact without slipping, the magnitude of the tangential force $F_{c,x}$ must be less than $\mu F_{c,y}$, i.e. :

$$|F_{c,x}| < |\mu F_{c,y}| \quad (7)$$

where μ is the coefficient of friction. From Fig.2(c), we can get

$$F_{c,x} = F \sin \theta \quad (8)$$

$$F_{c,y} = F \cos \theta \quad (9)$$

Substituting equation (8) and (9) into (7), we have

$$|\tan \alpha| = \left| \frac{x}{y_0} \right| < \mu \quad (10)$$

That means a step must be taken before the point mass deviates from the foot with a magnitude of μy_0 . In order to change the orbit energy with a larger value, we let the foot change its location when the point mass arrives at X , and set

$$X = 0.5 \mu y_0 \quad (11)$$

Second, due to the restriction of the actuator, there is a lower limit to the time between steps (foot location changes), T_{min} , which models the practical actuation ability of swing leg.

From X and T_{min} , we can get the upper limit of the orbit energy:

$$E_{max} = \frac{2gX^2 e^{\frac{T_{min}}{T_c}}}{y_0 \left(e^{\frac{T_{min}}{T_c}} - 1 \right)^2} \quad (12)$$

From equation (3) and (4), we have

$$E^- = \frac{1}{2} \dot{x}_c^2 - \frac{g}{2y_0} X^2 = \frac{1}{2} (\dot{x}|_{x=0})^2 \quad (13)$$

In equation (5), we let

$$E^+ = E_{des} = \frac{1}{2} \dot{x}_c^2 - \frac{g}{2y_0} L_{des}^2 \quad (14)$$

From equation (13) and (14), we can have:

$$L_{des} = \pm \sqrt{\frac{2y_0}{g} \left[\frac{1}{2} (\dot{x}|_{x=0})^2 + \frac{g}{2y_0} X^2 - E_{des} \right]} = \pm \sqrt{E_a} \quad (15)$$

Note that, if

$$E_{des} \geq (\dot{x}|_{x=0})^2 + \frac{g}{y_0} X^2 \quad (16)$$

there will not be a positive solution for L_{des} , that means the desired orbit energy is much larger than the current value, so that just take only one step can't let the point mass move with the desired orbit energy. In this situation our strategy is increasing the orbit energy step by step.

If L_{des} , calculated from equation (15), is larger than μy_0 , i.e.

$$L_{des} \geq \mu y_0 \quad (17)$$

Which means the desired orbit energy is much less than the current value, so that a long step must be taken, which may violate the restriction on contact force. In this situation our strategy is decreasing the orbit energy step by step.

From the viewpoint of natural human walking, it's desirable that the swing foot always lands in front of the body. Considering all the conditions as (11), (12), (16) and (17), we design L_{des} as

$$L_{des} = \begin{cases} 0.6X, & E_a \leq 0 \text{ or } \sqrt{E_a} \leq 0.6X \\ 1.6X, & \sqrt{E_a} \geq 1.6X \\ \sqrt{E_a}, & 0.6X < \sqrt{E_a} < 1.6X \end{cases} \quad (18)$$

Theorem 1 : For the 2D LIPM with point foot, a foot placement controller as shown in equations (11) and (18) can control the point mass move from any permitted state (i.e. the orbit energy is less than the upper limit) into a desired periodic gait (i.e. the orbit energy is equal to the desired one with a permitted value) with contact consistency.

Theorem 1 means when the point mass even suffers a sudden disturbance (e.g. a sudden push) during the motion, if the orbit energy doesn't exceed E_{max} , the designed foot placement controller can stabilize the motion.

Equation (11) answers the question: when a step should be taken? Which prevents the contact consistency during walking. And equation (18) answers the question: where the foot should be placed? Which achieves a desired walking cycle.

3. ONLINE TRAJECTORIES PLANNING IN TASK SPACE

In this section we will discuss the planning of the desired trajectories in task space during biped walking based on the foot placement controller in section 2.

As mentioned above, the torso's pitch angle and the hip's height should be stabilized to constants during walking. Additionally, the swing leg plays an indispensable role, and its main task includes taking off from the ground, moving forward and landing to a deliberate location, and then via changing its role as a stance leg to continue the walking. So the task space during biped walking can be selected as:

$$P_{tsk} = [\theta; y_{hip}; x_{swt}; y_{swt}] \quad (19)$$

where θ is the pitch angle of the torso, y_{hip} is the height of the hip, x_{swt} and y_{swt} are the horizontal and vertical component of the position of the swing foot. It's clear that the tasks in (19) are linearly independent.

The desired pitch angle of the torso and the height of the hip are set as:

$$\begin{cases} \theta_{des} = \dot{\theta}_{des} = \ddot{\theta}_{des} = 0 \\ y_{hip}^{des} = H = constant, \quad \dot{y}_{hip}^{des} = \ddot{y}_{hip}^{des} = 0 \end{cases} \quad (20)$$

Figure 4 illustrates a desired stance phase during walking. The hip moves as a 2D LIP, and P is the desired location where the stance foot should be placed in next stance phase calculated by equation (18). The dash-dotted line denotes the desired trajectory of the swing foot. The trajectories can be planned as a function of time [11, 18] or the geometric evolution of the biped [19, 20]. In order to withstand a disturbance robustly the latter option is adopted in this paper. During walking, the horizontal location of hip x_{hip} is monotonically increasing, so it can be selected as the parameter of desired trajectories.

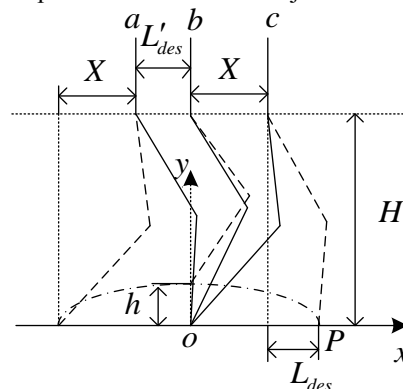


Figure 4. A desired stance phase contains three crucial moments: (a), the beginning of a stance phase, i.e. the moment just after the swing leg became the stance leg; (b), the moment when the hip passes through the stance point; (c), the moment when the hip arrives at X . The dashed line denotes the swing leg and the solid line denotes the stance leg.

Let $P_{swt}^{des} = [x_{swt}^{des}(x_{hip}); y_{swt}^{des}(x_{hip})]$ be the desired position of the swing foot in the local frame located at the point foot. There are three crucial moments in one stance phase as shown in Fig.4.

The constraint equations for the desired trajectories are described as follows:

(a). The beginning of a stance phase:

$$P_{swt}^{des}(-L'_{des}) = \begin{bmatrix} x_{swt}^{des}(-L'_{des}) \\ y_{swt}^{des}(-L'_{des}) \end{bmatrix} = \begin{bmatrix} -L'_{des} - X \\ 0 \end{bmatrix} \quad (21)$$

$$\dot{P}_{swt}^{des}(-L'_{des}) = \begin{bmatrix} \dot{x}_{swt}^{des}(-L'_{des}) \\ \dot{y}_{swt}^{des}(-L'_{des}) \end{bmatrix} = \begin{bmatrix} 0 \\ 0 \end{bmatrix} \quad (22)$$

(b). The moment when the hip pass through the stance point: (Let h be the maximum clearance of the swing leg):

$$P_{swt}^{des}(0) = \begin{bmatrix} x_{swt}^{des}(0) \\ y_{swt}^{des}(0) \end{bmatrix} = \begin{bmatrix} 0 \\ h \end{bmatrix} \quad (23)$$

$$\dot{P}_{swt}^{des}(0) = \begin{bmatrix} \dot{x}_{swt}^{des}(0) \\ \dot{y}_{swt}^{des}(0) \end{bmatrix} = \begin{bmatrix} v \\ 0 \end{bmatrix}, v \geq 0 \quad (24)$$

(c). The moment when the hip arrives at X :

$$P_{swt}^{des}(X_{max}) = \begin{bmatrix} x_{swt}^{des}(X) \\ y_{swt}^{des}(X) \end{bmatrix} = \begin{bmatrix} X + L_{des} \\ 0 \end{bmatrix} \quad (25)$$

$$\dot{P}_{swt}^{des}(X_{max}) = \begin{bmatrix} \dot{x}_{swt}^{des}(X) \\ \dot{y}_{swt}^{des}(X) \end{bmatrix} = \begin{bmatrix} 0 \\ 0 \end{bmatrix} \quad (26)$$

Using a sinusoidal function of x_{hip} , the desired trajectory of swing foot is planned as follows:

$$x_{swt}^{rd}(x_{hip}) = \begin{cases} (L'_{des} + X) \sin\left(\frac{\pi x_{hip}}{2L'_{des}}\right), x_{hip} \in [-L'_{des}, 0] \\ (L_{des} + X) \sin\left(\frac{\pi x_{hip}}{2X}\right), x_{hip} \in (0, X] \end{cases} \quad (27)$$

$$y_{swt}^{des}(x_{hip}) = \begin{cases} \frac{h}{2} + \frac{h}{2} \cos\left(\frac{\pi x_{hip}}{L'_{des}}\right), x_{hip} \in [-L'_{des}, 0] \\ \frac{h}{2} + \frac{h}{2} \cos\left(\frac{\pi x_{hip}}{X}\right), x_{hip} \in (0, X] \end{cases} \quad (28)$$

Where L_{des} and L'_{des} are the horizontal distance between the desired foot location and the hip in the current and the former step, respectively, as shown in Fig. 4.

4. ROBOT MODEL AND TASK SPACE CONTROLLER

In this section, the dynamics of a planar 5-link point foot biped is introduced and a task space controller based on the dynamics model is designed to realize the trajectories presented by (20),(27)and (28).

As shown in Fig.2.(b), if there is no motion between the stance foot and the ground [2, 6, 10, 21], and the origin of the local reference frame is located at the point foot, a set of generalized coordinate of the biped robot can be selected as:

$$q_e = [q_r; \theta] \quad (29)$$

Where $q_r = [\theta_{1r}; \theta_{2r}; \theta_{2l}; \theta_{1l}]$ is the joint configuration of the robot. and θ is the pitch angle of the torso in the local frame.

Using the Lagrange method, we can get the dynamics of the robot[22]:

$$M(q_e) \ddot{q}_e + C(\dot{q}_e, q_e) \dot{q}_e + G(q_e) = S^T \tau \quad (30)$$

where $M(q_e) \in R^{5 \times 5}$ is the inertia matrix of the robot, $C(\dot{q}_e, q_e) \in R^{5 \times 5}$ is the centripetal and Coriolis forces, $G(q_e) \in R^{5 \times 1}$ is the gravity forces, $S = [I_{4 \times 4} \quad 0_{4 \times 1}]$ is the selecting matrix of the actuated joints, $\tau \in R^{4 \times 1}$ is the vector of actuated joint torques.

Let $P_{tsk} = f(q_e)$, the task velocities can be calculated as:

$$\dot{P}_{tsk} = \frac{\partial f}{\partial q_e} \dot{q}_e = J_{tsk} \dot{q}_e \quad (31)$$

If $rank(J_{tsk}) = 4$, by using the Moore-Penrose pseudo-inverse of the task Jacobian[23]:

$$\dot{q}_e = J_{tsk}^{\#} \dot{P}_{tsk} \quad (32)$$

$$\ddot{q}_e = J_{tsk}^{\#} \ddot{P}_{tsk} + \frac{d(J_{tsk}^{\#})}{dt} \dot{P}_{tsk} \quad (33)$$

where $J_{tsk}^{\#} = J_{tsk}^T (J_{tsk} J_{tsk}^T)^{-1}$. Substituting (32) and (33) into (30), the dynamics in task space can be expressed as:

$$M(q_e) J_{tsk}^{\#} \ddot{P}_{tsk} + \left[C(\dot{q}_e, q_e) J_{tsk}^{\#} + \frac{d(J_{tsk}^{\#})}{dt} \right] \dot{P}_{tsk} + G(q_e) = S^T \tau \quad (34)$$

Multiplying equation (34) by S :

$$\tilde{M} \ddot{P}_{tsk} + \tilde{C} \dot{P}_{tsk} + \tilde{G} = \tau \quad (35)$$

where $\tilde{M} = S M(q_e) J_{tsk}^{\#}$, $\tilde{C} = S \left[C(\dot{q}_e, q_e) J_{tsk}^{\#} + M(q_e) \frac{d(J_{tsk}^{\#})}{dt} \right]$, $\tilde{G} = S G(q_e)$.

Equation (35) means the full dynamics of the robot can be represented by the top portions of the equation (34)[10]. A task space PD type controller can be designed as:

$$\tau = \tilde{M} \ddot{P}_{tsk}^{des} + \tilde{C} \dot{P}_{tsk} + \tilde{G} - \tilde{M} (K_P e_{tsk} + K_D \dot{e}_{tsk}) \quad (36)$$

Where $e_{tsk} = P_{tsk} - P_{tsk}^{des}$, $\dot{e}_{tsk} = \dot{P}_{tsk} - \dot{P}_{tsk}^{des}$.

Note that the controller (36) doesn't need to calculate the inversion of inertial matrix, which is more convenient than the method of [13, 14]. And it is similar to the controllers of [10, 21], in which the task space Jacobian should take the contact constraints into account. Here the contact constraints are considered in equation (30), thus the controller is more convenient to implement.

5. SIMULATION AND DISCUSSIONS

Simulation experiments are implemented in MATLAB. By using the "SimMechanics" toolbox, a virtual 5-link planar biped robot with two symmetric legs is built as shown in Fig.5. The physical parameters of the robot are shown in Table 1, and walking is beginning with the initial states shown in Table 2.

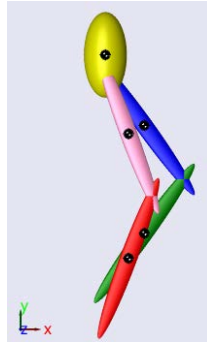


Figure 5. A virtual 5-link planar biped robot

Table 1. Physical parameters of the virtual biped robot

Model parameter	Units	Torso	Thigh	Shank
Mass	kg	18.84	5.024	5.024
Length	m	0.3	0.4	0.4
Inertia	kg · m ²	0.2041	0.06766	0.06766
Mass center to the joint	m	0.1	0.2	0.2

Table 2. Initial states of the virtual biped robot. Set the right leg as the stance leg initially.

	θ_{1r}	θ_{2r}	θ_{1l}	θ_{2l}	θ	x_{hip}	y_{hip}	x_{swt}	y_{swt}
q (rad, m)	0.7108	-0.3554	0.9578	-0.4789	0	0	0.75	0	0.04
\dot{q} (rad/s, m/s)	0	0	0	0	0	0	0	0	0

In simulation, we set the desired height of hip $H = 0.75m$. With different desired orbital energies ($E_{des} = 0$ and $E_{des} = 0.5$), the simulation results validate the online walking pattern generating method and the task space controller. A horizontal disturbance with magnitude of 100N is imposed on the center of the torso at 2.5s, and it lasts for 0.1s. A nonlinear compliant contact model with Coulomb friction is used to model the contact forces between the robot's foot and the ground as described in[4, 24].

Fig. 6 shows the orbit energy of the hip in 8 seconds. With the initial configuration in Table 2, the robot's COM is locating at the right side of the stance point, due to the gravity the robot will move forward, that is the primary actuation of the walking. So even when the hip's orbit energy is zero, the robot will not come to a stop as the blue line shown in Fig.6. It can be found that the orbit energy of the hip is not a constant during any stance phase. That is because the legs are not massless, especially the swing leg. While the ideal LIPM assumes the legs are massless. Nevertheless, the robot walks with a periodic gait even suffering the sudden disturbance.

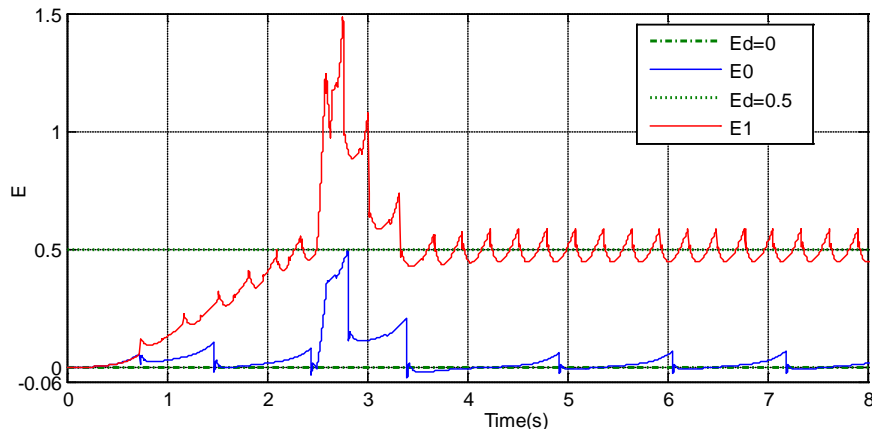


Figure.6 The orbit energy of the hip during walking. The green lines denote the desired orbit energy. The solid lines denote the orbit energy of the hip

The tangential component of the contact force of the right foot during walking is shown in Fig.7 with solid lines, and the green dashed lines denote the bound of friction force which is calculated by multiplying the normal component of the contact force with the coefficient of friction used in the contact model. When the solid lines (red or blue) locate inside the range formed by the zero grid line and the green dashed line, it means the friction force locate inside the friction cone, thus the contact consistency is preserved.

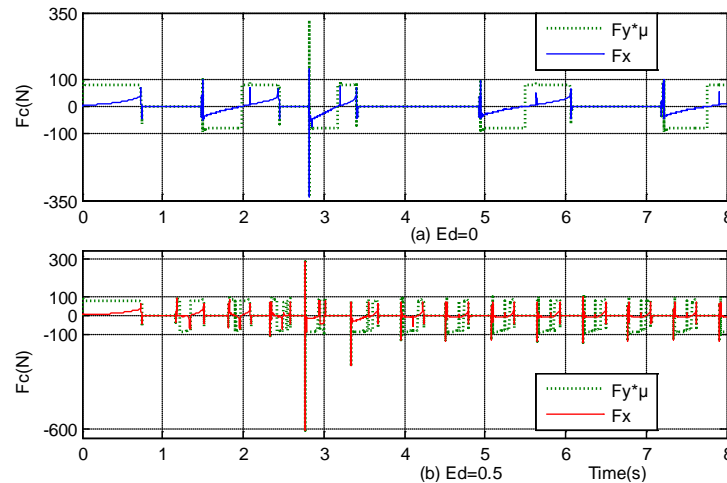


Figure 7. Effects of selecting different switching under dynamic condition

Considering the practical restriction of the actuators, in simulation we impose upper and lower limits on the actuation torques as shown in Fig.8 and Fig.9.

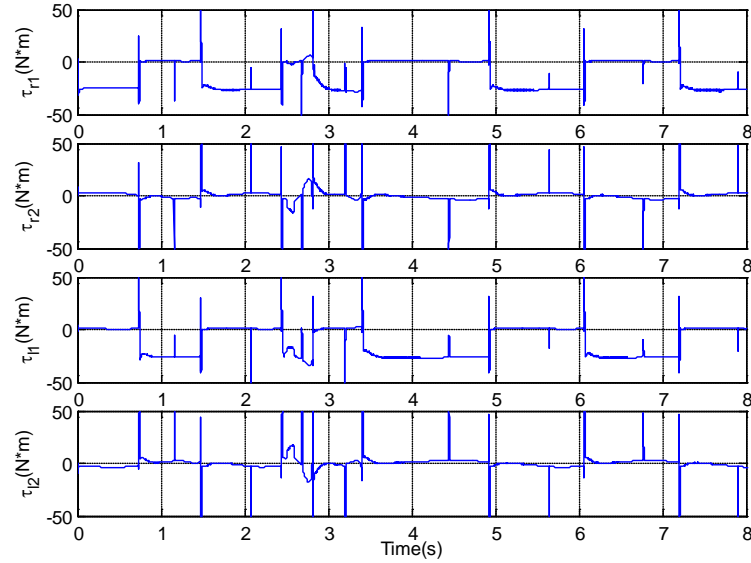


Figure 8. Actuation torque of each link during walking when $E_{des} = 0$

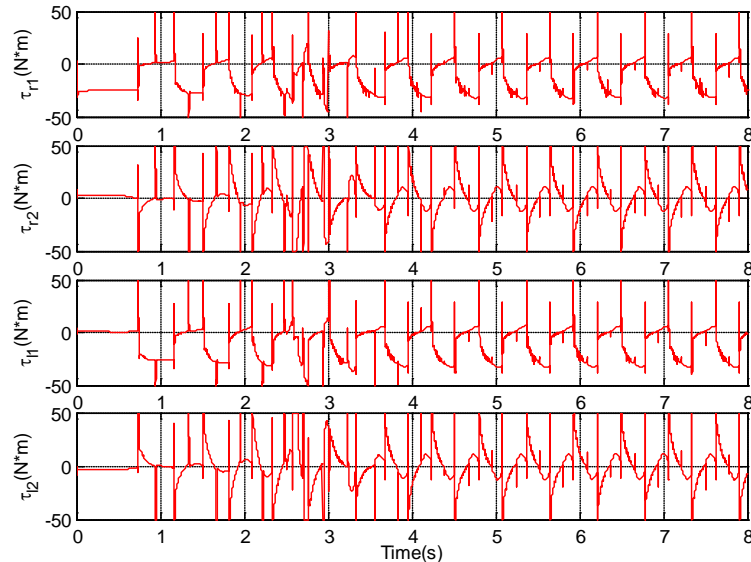


Figure 9. Actuation torque of each link during walking when $E_{des} = 0.5$

6. CONCLUSION

In this paper, we address the issue of walking control of a planar biped robot with contact consistency. By modeling the motion of the hip as a 2D-LIPM, a foot placement controller which can preserve the contact consistency is proposed to track the desired orbit energy. By selecting the hip's horizontal locomotion as the parameter, the walking pattern is generated on the real time. A task space PD type controller without calculating the inversion of inertial matrix is designed to realize the biped walking. Simulation result shows the proposed method not only can control the robot walking into periodic gait, but also can withstand a sudden disturbance. The future work will focus on extending the method into a 3D biped robot.

ACKNOWLEDGEMENTS

This work has been funded by the Crossing Specialties Co-educating Program for PhD students in National University of Defense Technology(No.kxk140101), and the National High Technology Research and Development Program of China(No.2011AA040801).

APPENDIX

A. Proof of theorem 1:

Case 1:

When $E_a \leq 0$ or $\sqrt{E_a} \leq 0.6X$, let $L_{des} = 0.6X$, substitute it into equation (6)

$$\Delta E = E^+ - E^- = \frac{0.32g}{y_0} X^2 = constant \quad (37)$$

That means when the current orbit energy is much less than the desired one, we take a step such that the orbit energy increase with a constant value. For the desired orbit energy is finite, so after taking finite steps, e.g. N , we can have:

$$\Delta E_N = E_{des} - E_N \in \left[0, \frac{0.32g}{y_0} X^2 \right) \quad (38)$$

where E_N is the orbit energy when $N(1,2,\dots)$ steps have been taken. Then we have:

$$\sqrt{E_a} = \sqrt{\frac{2y_0}{g}(E_N - E_{des}) + X^2} \in (0.6X, X] \quad (39)$$

For the next step the point mass will come to case 3.

Case 2:

When $\sqrt{E_a} \geq 1.6X$, let $L_{des} = 1.6X$, substitute it into equation(6):

$$\Delta E = E^+ - E^- = -\frac{0.78g}{y_0} X^2 = constant \quad (40)$$

That means when the current orbit energy is much bigger than the desired one, we take a step such that the orbit energy decrease with a constant value. For the desired orbit energy is finite, so after taking finite steps, e.g. M , we can have:

$$\Delta E_M = E_{des} - E_M \in \left(-\frac{0.78g}{y_0} X^2, 0 \right] \quad (41)$$

where E_M is the orbit energy when $M(1,2,\dots)$ steps have been taken. Then we have:

$$\sqrt{E_a} = \sqrt{\frac{2y_0}{g}(E_M - E_{des}) + X^2} \in [X, 1.6X) \quad (42)$$

For the next step the point mass will come to case 3, too.

Case 3:

When $0.6X < \sqrt{E_a} < 1.6X$, let $L_{des} = \sqrt{E_a}$, substitute equation (15) into(6):

$$\Delta E = E^+ - E^- = 0 \quad (43)$$

That means when the point mass take a step to the desired location, the orbit energy will be equal to the desired one.

From equation (15), we can see that when the current orbit energy is equal to the desired one, $L_{des} \equiv X$ Then from equation (3), $\dot{x}|_{x=X} \equiv constant$, and then from equation(45), the period of stance phase is a constant too.

Note that no matter the cases,

$$0.6X \leq L_{des} \leq 1.6X = 0.8\mu y_0 \quad (44)$$

That means the contact force restriction(10) will always be satisfied.

Above all, we can conclude that the designed X and L_{des} can control the point mass move from any permitted state into a period gait with contact consistency.

B. Derivation of the maximum value of orbit energy E_{max}

Given an initial state $(x(0), \dot{x}(0))$ and the final state $(x(t), \dot{x}(t))$, the transition time can be caculated as [17]:

$$t = T_c \ln \frac{x(t) + T_c \dot{x}(t)}{x(0) + T_c \dot{x}(0)} \quad (45)$$

where $T_c = \sqrt{\frac{y_0}{g}}$. Note that the two states must have a same orbit energy, i.e.

$$\frac{1}{2}\dot{x}(0)^2 - \frac{g}{2y_0}x(0)^2 = \frac{1}{2}\dot{x}(t)^2 - \frac{g}{2y_0}x(t)^2 \quad (46)$$

Supposing the point mass is locating at $-X$, moving toward the foot with the permitted maximum velocity \dot{X} , after T_{min} , it will arrive at X with the permitted maximum velocity \dot{X} , from equation(45), we have

$$T_{min} = T_c \ln \left(\frac{X + T_c \dot{X}}{-X + T_c \dot{X}} \right) \quad (47)$$

Solving \dot{X} in (47)

$$\dot{X} = \frac{\left(e^{\frac{T_{min}}{T_c}} + 1 \right) X}{\left(e^{\frac{T_{min}}{T_c}} - 1 \right) T_c} \quad (48)$$

From equation (3), the permitted maximum value of the orbit energy is

$$E_{max} = \frac{2gX^2 e^{\frac{T_{min}}{T_c}}}{y_0 \left(e^{\frac{T_{min}}{T_c}} - 1 \right)^2} \quad (49)$$

REFERENCES

- [1] T. d. Boer, *Foot placement in robotic bipedal locomotion*, Delft University, Ph.D., 2012
- [2] J. W. Grizzle, G. Abba and F. Plestan, "Asymptotically Stable Walking for biped robot: analysis via systems with impulse effects", *IEEE Transactions on automatic control*, Vol.46, pp. 51-64, 2001
- [3] G. Song and M. Zefran, "Underactuated dynamic three-dimensional bipedal walking", *Proceedings of the 2006 IEEE International Conference on Robotics and Automation*, pp. 854-859, 2006
- [4] M. Azad and R. Featherstone, "Balancing and hopping motion of a planar hopper with one actuator", *IEEE International Conference on Robotics and Automation (ICRA)*, pp. 2019-2024, 2013
- [5] M. Vukobratovic, "ZMP: a review of some basic misunderstandings", *International Journal of Humanoid Robotics*, Vol.3, pp. 153-175, 2006
- [6] E. R. Westervelt, J. W. Grizzle and D.E.Koditschek, "Hybrid Zero Dynamics of Planar Biped Walker", *IEEE Transactions on automatic control*, Vol.48, pp. 42-56, 2003
- [7] E. R. Westervelt, G. Buche and J.W Grizzle, "Inducing dynamically stable walking in an underactuated prototype planar biped", *Proceedings of the 2004 IEEE International Conference on Robotics and Automation*, pp. 4234-4239, 2004
- [8] L. Sentis and O. Khatib, "Synthesis of whole-body behaviors through hierarchical control of behavioral primitives", *International Journal of Humanoid Robotics*, Vol.2, pp. 505-518, 2005
- [9] M. Mistry, J. Nakanishi, G. Cheng and S. Schaal, "Inverse kinematics with floating base and constraints for full body humanoid robot control", *2008 8th IEEE-RAS International Conference on Humanoid Robots*, pp. 22-27, 2008
- [10] M. Mistry, J. Buchli and S. Schaal, "Inverse dynamics control of floating base systems using orthogonal decomposition", *Proceedings of the 2010 IEEE International Conference on Robotics and Automation*, pp. 3406-3412, 2010
- [11] S. Faraji, S. Pouya, R. Moeckel and A. J. Ijspeert, "Compliant and adaptive control of a planar monopod hopper in rough terrain", *IEEE International Conference on Robotics and Automation (ICRA)*, Vol.pp. 4803-4810, 2013
- [12] L. Righetti, J. Buchli, M. Mistry and S. Schaal, "Inverse dynamics control of floating-base robots with external constraints: a unified view", *IEEE International Conference on Robotics and Automation (ICRA)*, pp.1085-1090, 2011
- [13] M. Mistry and L. Righetti, "Operational space control of constrained and underactuated systems", *Proceedings of Robotics: Science and Systems*, 2011
- [14] J. Park and O. Khatib, "Contact consistent control framework for humanoid robots", *Proceedings of the 2006 IEEE International Conference on Robotics and Automation*, pp. 1963-1969, 2006
- [15] S. Kajita and K. Tani, "Study of Dynamic Biped Locomotion on Rugged Terrain-Theory and Basic Experiment", *Proceeding of 5th ICAR*, pp. 1991
- [16] S. Kajita, F. Kanehiro, K. Kancko, K. Yokoi and H. Hirukawa, "The 3D linear inverted pendulum model: a simple modeling for a biped walking pattern generation", *Proceedings of the 2001 IEEE/RSJ International Conference on Intelligent Robots and Systems*, Vol.1, pp. 239-246, 2001
- [17] *Humanoid Robots(Chinese language edition)*, (Beijing, China: Tsinghua University Press, 2007)

-
- [18] X. Mu, *Dyanmics and motion regulation of a five-link biped robot walking in the sagittal plane*, Department of Mechanical and Manufacturing Engineering, The University of Manitoba Winnipeg, Doctor of philosophy, 2004
- [19] C. Fu, M. Shuai, Y. Huang, J. Wang and K. Chen, "Parametric walking patterns and optimum atlases for underactuated biped robots", *Proceedings of the 2006 IEEE/RSJ International conference on intelligent robots and systems*, pp. 342-347, 2006
- [20] D. L. Wight, *A foot placement strategy for robust bipedal gait control*, University of Waterloo, Doctor of Philosophy, 2008
- [21] J. Nakanishi, M. Mistry and S. Schaal, "Inverse dynamics control with floating base and constraints", *Proceedings of the 2007 IEEE International Conference on Robotics and Automation*, pp. 1942-1947, 2007
- [22] *Feedback Control of Dynamic Bipedal Robot Locomotion*, (Boca Raton: Taylor & Francis Group, LLC, 2007)
- [23] M. Mistry, J. Nakanishi and S. Schaal, "Task space control with prioritization for balance and locomotion", *IEEE/RSJ ICIRS*, pp. 2007
- [24] M. Azad and R. Featherstone, "Modeling the contact between a rolling sphere and a compliant ground plane", *Australasian Conference Robotics and Automation*, pp. 2010